Relativistic analysis of field-kinetic and canonical electromagnetic systems

Cheyenne J. Sheppard and Brandon A. Kemp

Phys. Rev. A **93**, 053832 — Published 26 May 2016

DOI: 10.1103/PhysRevA.93.053832

Relativistic analysis of field-kinetic and canonical electromagnetic systems

Cheyenne J. Sheppard[1] and Brandon A. Kemp[2*]
[1] *College of Sciences and Mathematics, Arkansas State University, Arkansas 72467, USA*
[2] *College of Engineering, Arkansas State University, Arkansas 72467, USA*

We demonstrate the relativistic electromagnetic force and power distributions of the field-kinetic and canonical electromagnetic subsystems with respect to light normally incident upon a moving, lossless magneto-dielectric slab of material. Time average and time varying studies are preformed to demonstrate the continuum mathematical approach and discern between the physical characteristics of both field-kinetic and canonical subsystems. It is shown that when considering time average fields, both subsystems are equivalent, and thereby yield equivalent electromagnetic force and power results. The time varying case demonstrates the differences between the field-kinetic and canonical subsystems, where the field-kinetic subsystem attempts to distort the media, and the canonical subsystem satisfies global conservation principles.

PACS numbers: 03.30.+p, 03.50.De, 45.20.df, 42.25.Gy

I. INTRODUCTION

Originating in the early 1900's, optical momentum within media has been under question regarding mathematically exact momentum models [1]. The controversy began when two independent electromagnetic stress-energy-momentum (SEM) tensors were postulated for the mathematical modeling of light within materials [2, 3]. From the proposed SEM tensors, the momentum density expressions were defined as being either $\bar{D} \times \bar{B}$ [2] or $\epsilon_0 \mu_0 \bar{E} \times \bar{H}$ [3], where $\bar{D}$ and $\bar{B}$ represent the electric displacement and magnetic induction fields, $\bar{E}$ and $\bar{H}$ are the electric and magnetic fields, and ϵ_0 and μ_0 are the permittivity and permeability of vacuum, respectively. The former momentum density has been found to be the canonical momentum density, rendering the canonical momentum of a pulse of light within the medium. The latter momentum density is commonly known as the kinetic momentum density, where integration over the volume renders the kinetic momentum of a pulse of light within the medium [4]. In light of many theoretical and experimental findings, there still remains some confusion as to the complete theoretical description of the two physical interpretations of light within materials, specifically regarding the kinetic subsystem of light. However, significant theoretical advances have been made in recent years [4, 5].

The canonical momentum, $p_{can} = n\frac{\mathfrak{E}}{c}$, models the translations within or with respect to the medium and represents the combination of both field and material momentum values, where where n is the refractive index of the material, c is the speed of light in vacuum, and $\mathfrak{E}$ is the excitation energy [6]. Conversely, the kinetic momentum, $p_{kin} = \frac{1}{n}\frac{\mathfrak{E}}{c}$, models the center of mass translation of a material and represents the photon momentum void of material contributions. As is observed, each momentum model indicates that light experiences either an increase or decrease in momentum while propagating through a medium with refractive index, n [6]. Over the years, many researchers have reviewed the debate with many unique perspectives [7–19], however, a complete resolution has yet to be accepted.

Reviewing previous work on the kinetic subsystem led to the Balazs thought experiment [8]. Here, the thought experiment is conceptualized where a pulse with initial free space momentum, $p_i = \mathfrak{E}/c$, is incident onto an impedance matched slab of material, having thickness d. Within the material, the pulse is slowed by a path length $L = (n-1)d$, inducing a displacement difference with respect to the vacuum propagation path. Conservation principles invoke the slab gains linear momentum, giving rise to a material momentum, $p_m = \frac{\mathfrak{E}}{c}(1 - \frac{1}{n})$. As a consequence, momentum conservation requires that the momentum of the pulse be $p = \frac{1}{n}\frac{\mathfrak{E}}{c}$, corresponding to the kinetic momentum density $\bar{G} = \bar{E} \times \bar{H}/c^2$. We expand this thought experiment to include a relativistic analysis of a continuous wave. In doing so, we utilize both field-kinetic and canonical subsystem demonstrating the dynamics of light within media [5].

In this correspondence, we demonstrate the optical pressure exerted on a moving slab of magneto-dielectric material having velocity v at normal incidence. We make use of the Chu and Minkowski formulations to model the field-kinetic and canonical subsystems for each respective analysis. Within the analysis, we use both time average and time varying methods to study the total system with respect to both space and time. By use of energy and momentum conservation laws, we derive the optical work and pressure for each respective subsystem.

II. MATHEMATICAL FRAMEWORK

To analytically model systems, we utilize the subsystem concept prescribed by Penfield and Haus [7]. This allows one to partition a system to localize the force, power, energy, and momentum of the subsystem in question. The SEM tensor quantities related to the Chu and

* bkemp@astate.edu

Minkowski electromagnetic formulations are applied to model the field-kinetic and canonical systems, respectively [5]. However, we note that other leading formulation can be employed in attempt to model the dynamics of light [1, 5, 19].

A. Subsystem concept

The subsystem concept [7]

$$\varphi_j(\bar{r},t) = -\nabla\cdot\bar{S}_j(\bar{r},t) - \frac{\partial W_j(\bar{r},t)}{\partial t} \tag{1a}$$

$$\bar{f}_j(\bar{r},t) = -\nabla\cdot\bar{\bar{T}}_j(\bar{r},t) - \frac{\partial \bar{G}_j(\bar{r},t)}{\partial t} \tag{1b}$$

utilizes the energy and momentum continuity equations to divide up the total system into J subsystems, where $\bar{f}_j$ is the force density, φ_j is the power density, $\bar{\bar{T}}_j$ is the momentum flux or stress tensor, $\bar{S}_j$ is the power flux, $\bar{G}_j$ is the momentum density, and W_j is the energy density for any given subsystem j. This indicates that a subsystem may represent any arbitrary division of the total system (*i.e.* electromagnetic field, hydrostatic pressure, thermodynamic, etc). The conservation principles of the total closed system are stated

$$\sum_j \varphi_j(\bar{r},t) = 0 \tag{2a}$$

$$\sum_j \bar{f}_j(\bar{r},t) = 0 \tag{2b}$$

by closing each subsystem such that the sum of the energies and momenta for the overall system is zero. In general, the total force or power leaving any subsystem j within a given volume is found by integrating the force density, $\bar{f}_j$, and power density, φ_j, respectively. Thus, the total electromagnetic force and power are found such that

$$\bar{F}_e = -\int_V dV \frac{\partial}{\partial t}\bar{G}_e - \oint_A d\bar{A}\cdot\bar{\bar{T}}_e \tag{3a}$$

$$P_e = -\int_V dV \frac{\partial}{\partial t} W_e - \oint_A d\bar{A}\cdot\bar{S}_e. \tag{3b}$$

Here, the divergence theorem is employed to reduce the electromagnetic stress tensor, $\bar{\bar{T}}_e$, and power flux, $\bar{S}_e$, to a surface integral which is integrated over surface A enclosing volume V, where V is any given volume of the total system. These results are mathematically exact. However, to generalize this to moving media, we transform Eqs.(3) to accommodate moving boundaries. This stems from how the presented partial time derivatives no longer commute with the respective volume integrations. Kinetic theory demonstrates [20]

$$\frac{d}{dt}\int_V dV\bar{X} = \int_V dV\frac{\partial \bar{X}}{\partial t} + \oint_A da(\bar{a}\cdot\bar{v})\bar{X}, \tag{4}$$

where $\bar{X}$ represents an arbitrary density function with $\bar{v}$ being the speed of the boundary interface. Rearranging this relation and applying it to Eqs.(3), we can rewrite the electrodynamic force and power equations as

$$\bar{F}_e = -\oint_A d\bar{a}\cdot\left\{\bar{\bar{T}}_e - \bar{v}\bar{G}_e\right\} - \frac{d}{dt}\int_V dV\,\bar{G}_e \tag{5a}$$

$$P_e = -\oint_A d\bar{a}\cdot\left\{\bar{S}_e - \bar{v}W_e\right\} - \frac{d}{dt}\int_V dV\,W_e. \tag{5b}$$

Here, application of Eqs.(5) render the electrodynamic subsystem for any arbitrary moving system. Additionally, by application of Eq.(4), one can transform Eqs.(5) to mathematically model specific systems, as will be discussed in the latter sections of this correspondence.

The time-average force and power expressions are found by applying standard definitions to Eqs.(5) such that

$$\langle\bar{F}\rangle_e = -\oint_A d\bar{a}\cdot\left\{\langle\bar{\bar{T}}\rangle_e - \bar{v}\langle\bar{G}\rangle_e\right\} \tag{6a}$$

$$\langle P\rangle_e = -\oint_A d\bar{a}\cdot\left\{\langle\bar{S}\rangle_e - \bar{v}\langle W\rangle_e\right\}. \tag{6b}$$

Due to the generalized nature of Eqs.(5), the resulting time average values, Eqs.(6), are the generalized time average expressions for any arbitrarily moving electromagnetic subsystem.

III. MATHEMATICAL ANALYSIS

In this section, a gedankenexperiment is used to demonstrate the force and power relations of a moving magneto-dielectric slab of material in both the time-average and time-varying perspectives. The prescribed conservation equations, demonstrated in Sec II, are used to validate the systems via statements of energy and momentum conservation. The Chu and Minkowski electromagnetic formulations [20, 21] are employed to illustrate the dynamics of the field-kinetic and canonical electromagnetic systems, respectively. This allows for the theoretical study of electromagnetic and material contributions, and how each system changes with respect to both space and time.

A. Time average

Consider an electromagnetic wave normally incident from vacuum onto a rigid, lossless, non-dispersive, isotropic magneto-dielectric slab, where an observer sees the slab of material moving along the z axis within vacuum, as in Fig 1. The slab has a given proper thickness, d, with the material boundaries defined at $z = vt$ and $z = vt + \gamma d$, where $\gamma = (1-\beta^2)^{-1/2}$ is the Lorentz factor, $\bar{v} = \hat{z}v$ is the velocity vector of the moving material, and $\beta = v/c$ is the normalized velocity quantity. We note that the slab thickness, $z_2 - z_1$, is derived to

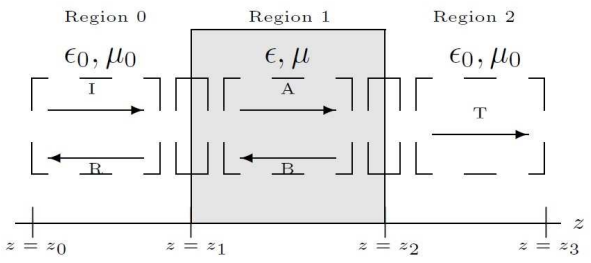

FIG. 1. A plane wave normally incident on a magneto-dielectric with refractive index $n = c\sqrt{\epsilon\mu}$, moving with velocity $v = zt$.

be γd for all inertial reference frames, where the inverse Lorentz transformation was used. The wave solutions are derived from the incident electric wave component, $\bar{\mathcal{E}}_i = \hat{x}E_0 e^{i(k_i z - \omega_i t)}$, where the incident wave is propagating along the positive $\hat{z}$ direction [21]. In this section, the time-averaged electromagnetic force and power are analyzed within the relativistically invariant field-kinetic and canonical formulations [5].

The Minkowski formulation is applied to present the time-average analysis. The incident Minkowski fields in the stationary frame are

$$\bar{\mathcal{E}}_i = \hat{x}E_0 e^{i(k_i z - \omega_i t)} \tag{7a}$$

$$\mathcal{H}_i = \hat{y}\frac{E_0}{c\mu_0} e^{i(k_i z - \omega_i t)} \tag{7b}$$

where, the incident wave vector is given as

$$\bar{k}_i = \hat{z}k_i = \hat{z}\frac{\omega_i}{c} \tag{8}$$

and subscript i represents the incident field relations. The reflected Minkowski fields, denoted by subscript r, in the stationary frame are

$$\bar{\mathcal{E}}_r = \hat{x}E_0 R e^{-i(k_r z + \omega_r t)} \tag{9a}$$

$$\bar{\mathcal{H}}_r = -\hat{y}\frac{E_0}{c\mu_0} R e^{-i(k_r z + \omega_r t)} \tag{9b}$$

where, the reflected wave vector is

$$\bar{k}_r = -\hat{z}k_r = -\hat{z}\frac{\omega_r}{c} \tag{10}$$

and R is the reflection coefficient. Within the moving slab, there are two wave coefficients denoted A and B. Here, coefficient A represents the amplitude of the wave propagating in the positive z direction where coefficient B represents the wave propagating along negative z direction. The Minkowski fields for the $+\hat{z}$ (positive) propagating wave within the material are denoted by subscript a, and are given as

$$\bar{\mathcal{E}}_a = \hat{x}AE_0 e^{i(k_a z - \omega_a t)} \tag{11a}$$

$$\bar{\mathcal{B}}_a = \hat{y}\frac{E_0}{c}\frac{n+\beta}{1+n\beta} A e^{i(k_a z - \omega_a t)} \tag{11b}$$

$$\bar{\mathcal{D}}_a = \hat{x}\frac{E_0}{c^2\mu'}\frac{n(n+\beta)}{1+n\beta} A e^{i(k_a z - \omega_a t)} \tag{11c}$$

$$\bar{\mathcal{H}}_a = \hat{y}\frac{n}{c\mu'} A E_0 e^{i(k_a z - \omega_a t)} \tag{11d}$$

where the associated wave vector is

$$\bar{k}_a = \hat{z}k_a = \hat{z}\frac{n+\beta}{1+n\beta}\frac{\omega_a}{c}. \tag{12}$$

Similarly, the relativistic Minkowski fields for the $-\hat{z}$ (negative) propagating wave within the material are denoted by subscript b, and are given as

$$\bar{\mathcal{E}}_b = \hat{x}E_0 B e^{-i(k_b z + \omega_b t)} \tag{13a}$$

$$\bar{\mathcal{B}}_b = -\hat{y}\frac{E_0}{c}\frac{n-\beta}{1-n\beta} B e^{-i(k_b z + \omega_b t)} \tag{13b}$$

$$\bar{\mathcal{D}}_b = \hat{x}\frac{E_0}{c^2\mu'}\frac{n(n-\beta)}{1-n\beta} B e^{-i(k_b z + \omega_b t)} \tag{13c}$$

$$\bar{\mathcal{H}}_b = -\hat{y}\frac{n}{c\mu'} B E_0 e^{-i(k_b z + \omega_b t)} \tag{13d}$$

where the associated wave vector is

$$\bar{k}_b = -\hat{z}k_b = -\hat{z}\frac{n-\beta}{1-n\beta}\frac{\omega_b}{c}. \tag{14}$$

For notational simplicity, we define the effective refractive indices for the $+\hat{z}$ and $-\hat{z}$ propagating waves in the medium as $n_a = (n+\beta)/(1+n\beta)$ and $n_b = (n-\beta)/(1-n\beta)$, respectively. The transmitted Minkowski fields in the stationary frame are

$$\bar{\mathcal{E}}_t = \hat{x}TE_0 e^{i(k_t z - \omega_t t)} \tag{15a}$$

$$\bar{\mathcal{H}}_t = \hat{y}\frac{E_0}{c\mu_0} T e^{i(k_t z - \omega_t t)} \tag{15b}$$

where the associated wave vector, k_t, is given as

$$\bar{k}_t = \hat{z}k_t = \hat{z}\frac{\omega_t}{c}. \tag{16}$$

Here, T represents the transmission coefficient and subscript t denotes the transmitted wave relations. We note that the general relations for wave vectors and electromagnetic field within moving media have been previously derived [5, 20, 21].

Here, we use standard boundary conditions to evaluate the field relations at each boundary [20]. Thus, employing tangential boundary conditions, given as

$$\hat{z} \times (\bar{\mathcal{E}} + \bar{v} \times \bar{\mathcal{B}}) = 0, \tag{17a}$$

$$\hat{z} \times (\bar{\mathcal{H}} - \bar{v} \times \bar{\mathcal{D}}) = 0, \tag{17b}$$

at both $z = vt$ and $z = vt + \gamma d$ while using algebraic techniques, the solutions for coefficients $A, B, R,$ and T

are found to be,

$$A = \frac{2\mu_r'(\mu_r'+n)(1+n\beta)}{(1+\beta)\left[(\mu_r'+n)^2-(\mu_r'-n)^2e^{i\theta}\right]} \tag{18a}$$

$$B = \frac{2\mu_r'(\mu_r'-n)(1-n\beta)}{(1+\beta)\left[(\mu_r'-n)^2-(\mu_r'+n)^2e^{-i\theta}\right]} \tag{18b}$$

$$R = \frac{(1-\beta)(\mu_r'+n)(\mu_r'-n)\left(1-e^{i\theta}\right)}{(1+\beta)\left[(\mu_r'+n)^2-(\mu_r'-n)^2e^{i\theta}\right]} \tag{18c}$$

$$T = \frac{4\mu_r' n e^{i\sigma_A}}{(\mu_r'+n)^2-(\mu_r'-n)^2e^{i\theta}}, \tag{18d}$$

where $\sigma_A = \gamma d(k_A - k_t)$ and $\theta = \gamma d(k_A + k_B)$.

Application of phase matching conditions [20]

$$\begin{aligned}\phi &\equiv k_i v - \omega_i \\ &= -k_r v - \omega_r \\ &= k_a v - \omega_a \\ &= -k_b v - \omega_b \\ &= k_t v - \omega_t.\end{aligned} \tag{19}$$

allows for each respective wave interacting at each specific boundary to have identical phases where the phases corresponding to the second boundary have the additional phase term ($\phi \pm k\gamma d$). However, manipulation of Eq.(19) allows one to find the incident, reflected and/or transmitted angular frequencies for each region in terms of the incident angular frequency, ω_i. Thus,

$$\omega_r = \frac{1-\beta}{1+\beta}\omega_i \tag{20a}$$

$$\omega_a = \frac{1+n\beta}{1+\beta}\omega_i = \frac{1-\beta}{1-n_a\beta}\omega_i \tag{20b}$$

$$\omega_b = \frac{1-n\beta}{1+\beta}\omega_i = \frac{1-\beta}{1+n_b\beta}\omega_i \tag{20c}$$

$$\omega_t = \omega_i. \tag{20d}$$

Here, Eq.(20d) demonstrates that the incident and transmitted waves share the same energy ($\hbar\omega$) and momentum ($\hbar\omega/c$) per photon. However, it is seen that when utilizing the relations of the incident, reflected, and transmitted energy and momentum relations of each free space photon, we find

$$\bar{p}_{photon} = \hat{z}\frac{\hbar}{c}\left[\omega_i + \omega_r r - \omega_t t\right] = \hat{z}\frac{2\hbar\omega_i}{c(1+\beta)}r \tag{21a}$$

$$\mathcal{E}_{photon} = \hbar\left[\omega_i - \omega_r r - \omega_t t\right] = \frac{2\beta\hbar\omega_i}{1+\beta}r, \tag{21b}$$

where $\bar{p}_{photon}$ and $\mathcal{E}_{photon}$ represent the free space energy and momentum acting on the material, and r and t are the reflected and transmitted probability densities of the photon at the barrier, respectively. Application of the work-energy theorem, $\bar{p}\cdot\bar{v} = \mathcal{E}$ yields

$$\hat{z}\frac{2\hbar\omega_i}{c(1+\beta)}r \cdot c\bar{\beta} = \frac{2\beta\hbar\omega_i}{1+\beta}r, \tag{22}$$

demonstrating conservation of energy and momentum for the free photons.

Reviewing Eqs. (20) from a classical, continuum perspective implies that when considering moving systems, there is a change in the standing wave frequency on one side of the slab which is proportional to the velocity of the slab, and thereby yields a net change in energy and momentum within the incident and transmitted regions around the moving slab of material. This difference in energy and momentum induces a net radiation pressure, corresponding to a non-zero net electromagnetic force and power, which is exerted on the material.

Using electromagnetic theory, the time average Minkowski force,

$$\langle\bar{F}_{elec}\rangle = \hat{z}\frac{E_0^2}{2c^2\mu_0}\frac{(1-\beta)}{(1+\beta)} \times \frac{2\left(n^2-\mu_r'^2\right)^2(1-\cos(\theta))}{\left((n^4+6n^2\mu_r^2+\mu_r'^4)-(n^2-\mu_r'^2)^2\cos(\theta)\right)} \tag{23}$$

is found by employing Eq. (6a) in conjunction with the Minkowski field relations presented in Table I. Similarly, the time average Minkowski power,

$$\langle P_{elec}\rangle = \frac{E_0^2}{2c\mu_0}\frac{(1-\beta)}{(1+\beta)} \times \frac{2\beta\left(n^2-\mu_r'^2\right)^2(1-\cos(\theta))}{\left((n^4+6n^2\mu_r^2+\mu_r'^4)-(n^2-\mu_r'^2)^2\cos(\theta)\right)} \tag{24}$$

is found by utilizing Eq. (6b) along with the presented field relations in Table I. Here, both Eq. (23) and (24) are demonstrated in Fig 2 and are rendered in terms of free space values of the electromagnetic subsystem. Analytically, the time average force and power contributions cancel within the slab cancel, thereby yielding equivalent electrodynamic relations between the field-kinetic and canonical subsystems. This implies one could utilize any relativistic electromagnetic formulation to calculate the derived force and power expressions.

Conservation of electromagnetic energy and momentum is validated by use of the mechanical power expression, $\langle\bar{F}\rangle\cdot\bar{v} = \langle P\rangle$ [15, 21], which is related to energy and momentum conservation by a time derivative where the velocity field is held constant. Here, it is easily observed that

$$\begin{aligned}\langle\bar{F}_{elec}\rangle\cdot\bar{v} &= \hat{z}\frac{E_0^2}{2c^2\mu_0}\frac{(1-\beta)}{(1+\beta)} \\ &\quad\times\frac{2\left(n^2-\mu_r'^2\right)^2(1-\cos(\theta))}{\left((n^4+6n^2\mu_r^2+\mu_r'^4)-(n^2-\mu_r'^2)^2\cos(\theta)\right)}\cdot\hat{z}c\beta \\ &= \frac{E_0^2}{2c\mu_0}\frac{(1-\beta)}{(1+\beta)} \\ &\quad\times\frac{2\beta\left(n^2-\mu_r'^2\right)^2(1-\cos(\theta))}{\left((n^4+6n^2\mu_r^2+\mu_r'^4)-(n^2-\mu_r'^2)^2\cos(\theta)\right)} \\ &= \langle P_{elec}\rangle,\end{aligned} \tag{25}$$

Region	$\langle T_{zz}\rangle$	$\langle G_z\rangle$	$\langle W\rangle$	$\langle S_z\rangle$
0	$\frac{E_0^2}{2c^2\mu_0}\left(1+\lvert R\rvert^2\right)$	$\frac{E_0^2}{2c^3\mu_0}\left(1-\lvert R\rvert^2\right)$	$\frac{E_0^2}{2c^2\mu_0}\left(1+\lvert R\rvert^2\right)$	$\frac{E_0^2}{2c\mu_0}\left(1-\lvert R\rvert^2\right)$
1	$\frac{E_0^2}{2c^2\mu_0}\frac{n}{\mu_r'}\left[n_a\lvert A\rvert^2+n_b\lvert B\rvert^2\right]$	$\frac{E_0^2}{2c^3\mu_0}\frac{n}{\mu_r'}\left[n_a^2\lvert A\rvert^2-n_b^2\lvert B\rvert^2\right]$	$\frac{E_0^2}{2c^2\mu_0}\frac{n}{\mu_r'}\left[n_a\lvert A\rvert^2+n_b\lvert B\rvert^2\right]$	$\frac{E_0^2}{2c^2\mu_0}\frac{n}{\mu_r'}\left[\lvert A\rvert^2-\lvert B\rvert^2\right]$
2	$\frac{E_0^2}{2c^2\mu_0}\lvert T\rvert^2$	$\frac{E_0^2}{2c^2\mu_0}\lvert T\rvert^2$	$\frac{E_0^2}{2c^3\mu_0}\lvert T\rvert^2$	$\frac{E_0^2}{2c\mu_0}\lvert T\rvert^2$

TABLE I. The derived field values for the Minkowski subsystem.

and the electromagnetic force and power are equal and consistent within the system, $\langle\bar{F}_{elec}\rangle\cdot\bar{v}-\langle P_{elec}\rangle=0$. Additionally, the electromagnetic and mechanical subsystems are equal and opposite such that the relativistic constraints are maintained within the closed system [15, 21]. This result invokes the given relations, $\langle\bar{F}_{elec}\rangle=-\langle\bar{F}_{mech}\rangle$ and $\langle P_{elec}\rangle=-\langle P_{mech}\rangle$ to satisfy global energy and momentum conservation, as seen in Eqs.(2b) and (2a).

Here, we note that the presented results are significant, yet ambiguous. This is due to the electromagnetic force and power values yielding relations that are independent of material contributions. In the following subsection, we study the electromagnetic force and power distributions of a moving slab with time varying field expressions. This serves to illustrate the differences in the field-kinetic and canonical subsystems within optical media.

B. Time varying

In this subsection, we reevaluate the electrodynamics of Sec III A while employing time varying field definitions. With this, we employ the Chu (field-kinetic) and Minkowski (canonical) formulations in modeling the electromagnetic subsystem.

To accurately model the given system, it is advantageous to modify continuity Eqs.(5a-5b) from the generalized force and power expressions. This is done by applying Eq.(4) to derive the necessary relations for each region of interest. To illustrate this, we divide the system into contributions within each region (R_0, R_1, R_2) and at each boundary (B_1, B_2), where each region and boundary is specified in Fig 1. This renders

$$\bar{F}_{R_0}=-\oint_{R_0}d\bar{a}\cdot\left\{\bar{\bar{T}}-\bar{v}\bar{G}\right\}-\frac{d}{dt}\int_{z_0}^{z_1^-}dz\,\bar{G}\quad(26a)$$

$$\bar{F}_{B_1}=-\oint_{B_1}d\bar{a}\cdot\left\{\bar{\bar{T}}-\bar{v}\bar{G}\right\}-\frac{d}{dt}\int_{z_1^-}^{z_1^+}dz\,\bar{G}\quad(26b)$$

$$\bar{F}_{R_1}=-\oint_{R_1}d\bar{a}\cdot\left\{\bar{\bar{T}}-\bar{v}\bar{G}\right\}-\frac{d}{dt}\int_{z_1^+}^{z_2^-}dz\,\bar{G}\quad(26c)$$

$$\bar{F}_{B_2}=-\oint_{B_2}d\bar{a}\cdot\left\{\bar{\bar{T}}-\bar{v}\bar{G}\right\}-\frac{d}{dt}\int_{z_2^-}^{z_2^+}dz\,\bar{G}\quad(26d)$$

$$\bar{F}_{R_2}=-\oint_{R_2}d\bar{a}\cdot\left\{\bar{\bar{T}}-\bar{v}\bar{G}\right\}-\frac{d}{dt}\int_{z_2^+}^{z_3}dz\,\bar{G}.\quad(26e)$$

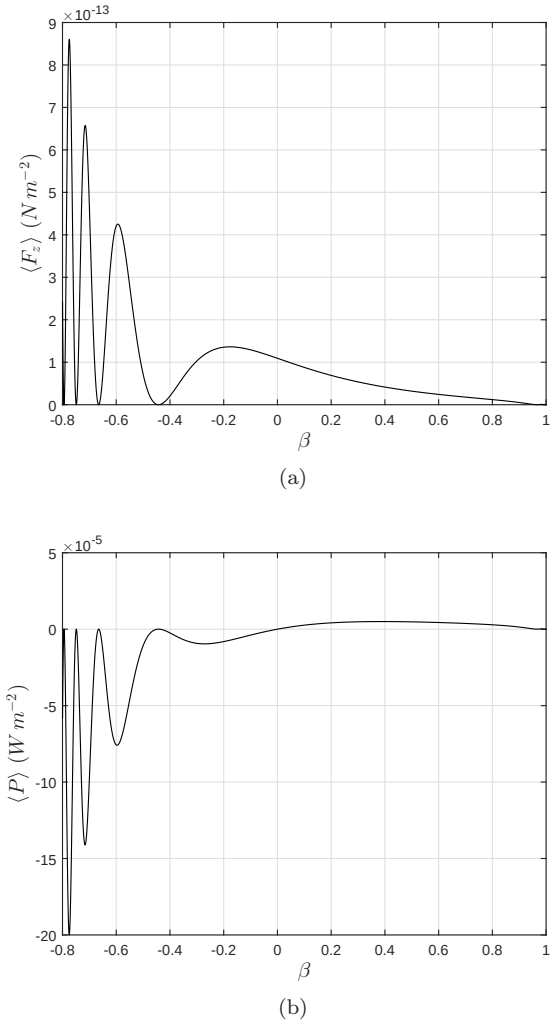

FIG. 2. The electromagnetic (a) force and (b) power versus velocity for the field-kinetic and canonical relativistic formulations are presented for a moving magneto-dielectric slab of thickness $d=\lambda_0/4n$. Here, the initial wavelength is $\lambda_0=640nm$, where $\epsilon=5\epsilon_0$, $\mu=3\mu_0$, $n=c\sqrt{\epsilon\mu}$, with $\beta=\frac{v}{c}$ as the normalized velocity.

where

$$\bar{F}=\bar{F}_{R_0}+\bar{F}_{B_1}+\bar{F}_{R_1}+\bar{F}_{B_2}+\bar{F}_{R_2}.\quad(27)$$

Here, superscripts + and − denote the evaluation of the given expression on the positive or negative side of a given point z. From this, it is easily seen that the volume inte-

gration of the momentum density within Eqs. (26b) and (26d) tends to zero, which is due to a vanishing volume integration at the boundary surface. Thus, by application of Eq.(4) into Eq.(26), the resulting force expressions for each respective region are

$$\bar{F}_{R_0} = -\oint_{R_0} d\bar{a}\cdot\bar{\bar{T}} - \int_{z_0}^{z_1^-} dz\,\frac{\partial\bar{G}}{\partial t} \tag{28a}$$

$$\bar{F}_{B_1} = -\oint_{B_1} d\bar{a}\cdot\left\{\bar{\bar{T}} - \bar{v}\bar{G}\right\} \tag{28b}$$

$$\bar{F}_{R_1} = -\oint_{R_1} d\bar{a}\cdot\bar{\bar{T}} - \int_{z_1^+}^{z_2^-} dz\,\frac{\partial\bar{G}}{\partial t} \tag{28c}$$

$$\bar{F}_{B_2} = -\oint_{B_2} d\bar{a}\cdot\left\{\bar{\bar{T}} - \bar{v}\bar{G}\right\} \tag{28d}$$

$$\bar{F}_{R_2} = -\oint_{R_2} d\bar{a}\cdot\bar{\bar{T}} - \int_{z_2^+}^{z_3} dz\,\frac{\partial\bar{G}}{\partial t}. \tag{28e}$$

Simplification of Eqs.(28) leads to the force expression

$$\bar{F}_j = -\oint_A d\bar{a}\cdot\left\{\bar{\bar{T}}_j^{out} - \bar{v}\bar{G}_j^{out}\right\} + \oint_A d\bar{a}\cdot\left\{\bar{v}\bar{G}_j^{in}\right\} - \int_V dV\,\frac{\partial\bar{G}_j^{in}}{\partial t} + \bar{F}_{R_0} + \bar{F}_{R_2}, \tag{29}$$

where superscript *out* represents field relations outside the slab of material while superscript *in* represents field relations inside the slab of material. Here, identical manipulations occur when solving the the total electromagnetic power expression. Thus, the power expression is given as

$$P_j = -\oint_A d\bar{a}\cdot\left\{\bar{S}_j^{out} - \bar{v}W_j^{out}\right\} + \oint_A d\bar{a}\cdot\left\{\bar{v}W_j^{in}\right\} - \int_V dV\,\frac{\partial W_j^{in}}{\partial t} + P_{R_0} + P_{R_2}. \tag{30}$$

Here, it is important to note that both Eqs.(5a-5b) and Eqs.(29-30) are equivalent, and will yield identical results in calculation.

1. *Minkowski*

Here, we present the time domain Minkowski fields derived from Eq.(A1), along with the complex fields in Eq.(7-15). Thus, the time domain incident Minkowski fields are

$$\bar{\mathcal{E}}_i = \hat{x}E_0\mathcal{I} \tag{31a}$$

$$\bar{\mathcal{H}}_i = \hat{y}\frac{E_0}{c\mu_0}\mathcal{I}. \tag{31b}$$

The reflected time domain Minkowski fields are

$$\bar{\mathcal{E}}_r = \hat{x}E_0\mathcal{R} \tag{32a}$$

$$\bar{\mathcal{H}}_r = -\hat{y}\frac{E_0}{c\mu_0}\mathcal{R}. \tag{32b}$$

The time domain Minkowksi fields for the positive propagating electromagnetic wave within the material are

$$\bar{\mathcal{E}}_a = \hat{x}E_0\mathcal{A} \tag{33a}$$

$$\bar{\mathcal{B}}_a = \hat{y}\frac{E_0}{c}\frac{n+\beta}{1+n\beta}\mathcal{A} \tag{33b}$$

$$\bar{\mathcal{D}}_a = \hat{x}\frac{E_0}{c^2\mu'}\frac{n(n+\beta)}{1+n\beta}\mathcal{A} \tag{33c}$$

$$\bar{\mathcal{H}}_a = \hat{y}\frac{n}{c\mu'}E_0\mathcal{A}. \tag{33d}$$

The time domain Minkowski fields for the negative propagating electromagnetic wave within the material are

$$\bar{\mathcal{E}}_b = \hat{x}E_0\mathcal{B} \tag{34a}$$

$$\bar{\mathcal{B}}_b = -\hat{y}\frac{E_0}{c}\frac{n-\beta}{1-n\beta}\mathcal{B} \tag{34b}$$

$$\bar{\mathcal{D}}_b = \hat{x}\frac{E_0}{c^2\mu'}\frac{n(n-\beta)}{1-n\beta}\mathcal{B} \tag{34c}$$

$$\bar{\mathcal{H}}_b = -\hat{y}\frac{n}{c\mu'}E_0\mathcal{B}. \tag{34d}$$

And the transmitted time domain Minkowski field are

$$\bar{\mathcal{E}}_t = \hat{x}E_0\mathcal{T} \tag{35a}$$

$$\bar{\mathcal{H}}_t = \hat{y}\frac{E_0}{c\mu_0}\mathcal{T}, \tag{35b}$$

where the values for $\mathcal{I}$, $\mathcal{R}$, $\mathcal{A}$, $\mathcal{B}$, and $\mathcal{T}$ are derived in Appendix A.

We utilize the force and power continuity expressions, Eqs. (29) and (30), alongside the Minkowski stress tensor, momentum density, energy density, and power flux, as previously defined, to derive the values for the time varying force and power of the canonical electromagnetic subsystem. Table II demonstrates the values utilized in calculation.

The time varying Minkowski force is given as

$$\bar{F}_M = \hat{z}\frac{E_0^2}{c^2\mu_0}[(\mathcal{I}^2+\mathcal{R}^2-\mathcal{T}^2) - \beta\{\mathcal{I}^2-\mathcal{R}^2-\mathcal{T}^2\}] + \hat{z}\frac{E_0^2}{c^3\mu_0}\frac{n}{\mu_r'}\Big\{v\left(n_a^2A^2(z_1^+) - n_b^2B^2(z_1^+)\right) - v\left(n_a^2A^2(z_2^-) - n_b^2B^2(z_2^-)\right) - n_a^2\int_{R_1} dz\frac{\partial\mathcal{A}^2}{\partial t} - n_b^2\int_{R_1} dz\frac{\partial\mathcal{B}^2}{\partial t}\Big\}, \tag{36}$$

where subscript M denotes the Minkowski electrodynamic subsystem. $\bar{F}_{R_0}$ and $\bar{F}_{R_2}$ render a null result. This is due to the stress tensor and momentum density integrations rendering equal and opposite forces, thereby canceling to provide a zero net force. This result also follows physical intuition, being that there is no electromagnetic force exerted on a vacuum. However, there is a nonzero electromagnetic force exerted within and on the boundaries of the given medium, as expressed in Eq.(36).

Expressions	Region 0	Region 1	Region 2
T_{zz}	$\frac{E_0^2}{c^2\mu_0}\left(\mathcal{I}^2+\mathcal{R}^2\right)$	$\frac{E_0^2}{c^2\mu_0}\frac{n}{\mu_r'}\left[n_a\mathcal{A}^2+n_b\mathcal{B}^2\right]$	$\frac{E_0^2}{c^2\mu_0}\mathcal{T}^2$
G_z	$\frac{E_0^2}{c^3\mu_0}\left(\mathcal{I}^2-\mathcal{R}^2\right)$	$\frac{E_0^2}{c^3\mu_0}\frac{n}{\mu_r'}\left[n_a^2\mathcal{A}^2-n_b^2\mathcal{B}^2\right]$	$\frac{E_0^2}{c^3\mu_0}\mathcal{T}^2$
W	$\frac{E_0^2}{c^2\mu_0}\left(\mathcal{I}^2+\mathcal{R}^2\right)$	$\frac{E_0^2}{c^2\mu_0}\frac{n}{\mu_r'}\left[n_a\mathcal{A}^2+n_b\mathcal{B}^2\right]$	$\frac{E_0^2}{c^2\mu_0}\mathcal{T}^2$
S_z	$\frac{E_0^2}{c\mu_0}\left(\mathcal{I}^2-\mathcal{R}^2\right)$	$\frac{E_0^2}{c^2\mu_0}\frac{n}{\mu_r'}\left[\mathcal{A}^2+\mathcal{B}^2\right]$	$\frac{E_0^2}{c\mu_0}\mathcal{T}^2$

TABLE II. The derived values for the time domain Minkowski subsystem.

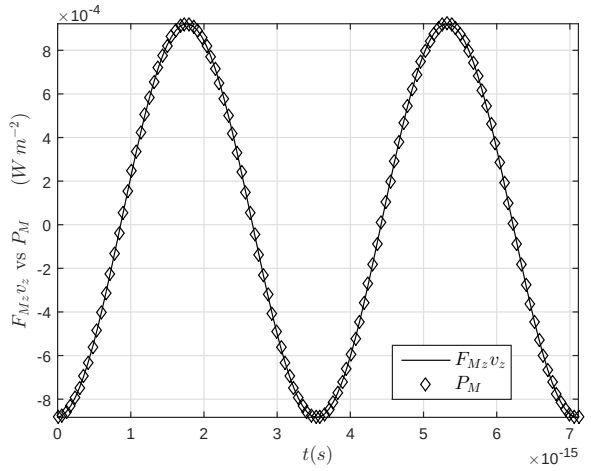

FIG. 3. The graphical representation of conservation, $\bar{F}_M\cdot\bar{v}=P_M$, in terms of the Minkowski formulation. Here, $\epsilon=5\epsilon_0$, $\mu=3\mu_0$, $n=\sqrt{\epsilon_r\mu_r}$, $\lambda_0=640nm$, $d=\lambda_0/4n$, and the velocity of the slab is $\bar{v}=\hat{z}7c/10$.

The time domain Minkowski power is derived as

$$\begin{aligned}P_M=&\frac{E_0^2}{c\mu_0}[(\mathcal{I}^2-\mathcal{R}^2-\mathcal{T}^2)+\beta\{\mathcal{I}^2+\mathcal{R}^2-\mathcal{T}^2\}]\\&+\frac{E_0^2}{c^2\mu_0}\frac{n}{\mu_r'}\Bigg\{v\left(n_aA^2(z_1^+)+n_bB^2(z_1^+)\right)\\&-v\left(n_aA^2(z_2^-)+n_bB^2(z_2^-)\right)-n_a\int_{R_1}dz\frac{\partial\mathcal{A}^2}{\partial t}\\&+n_b\int_{R_1}dz\frac{\partial\mathcal{B}^2}{\partial t}\Bigg\}.\end{aligned}\tag{37}$$

Similarly, P_{R_0} and P_{R_2} both render null results due to cancelations within the power flux and energy density terms of each expression. Again this is result agrees with intuition, due to the fact the electromagnetic power does no work on vacuum.

Simplification of Eqs.(36) and (37) is somewhat impractical, and is due to the cumbersome nature of the real and imaginary wave coefficients constituting the wave relations. Alternatively, the results are plotted to demonstrate conservation within the system while performing the relation $\bar{F}\cdot\bar{v}=P$, where graphical representation is shown in Fig 3. As can be seen, the work-energy relation is satisfied. Thus, the Minkowski formulation satisfies the electrodynamic subsystem. In addition, we note that to satisfy the total system, there is an equal and opposite mechanical force and power such that $\bar{F}_M=-\bar{F}_{mech}$ and $P_M=-P_{mech}$. This allows for global conservation and satisfies relativistic constraints (*i.e* constant velocity) within the system.

2. Chu

The Chu fields are derived by using prescribed vector field tranformations [7, 21] and the Minkowski time domain fields. In addition, the Chu boundary conditions render identical results to that of the Minkowski formulation, thereby allowing for the use of Eqs.(A2) and (A7) in reexpressing the Chu field relations. The time domain incident Chu fields are

$$\bar{\mathcal{E}}_{Ci}=\hat{x}E_0\mathcal{I}\tag{38a}$$

$$\bar{\mathcal{H}}_{Ci}=\hat{y}\frac{E_0}{c\mu_0}\mathcal{I}.\tag{38b}$$

The time domain reflected Chu fields are

$$\bar{\mathcal{E}}_{Cr}=\hat{x}E_0\mathcal{R}\tag{39a}$$

$$\bar{\mathcal{H}}_{Cr}=-\hat{y}\frac{E_0}{c\mu_0}\mathcal{R}\tag{39b}$$

The time domain Chu fields propagating in the positive direction within the material are

$$\bar{\mathcal{E}}_{Ca}=\hat{x}\,\frac{\mu_r'+n\beta}{\mu_r'(1+n\beta)}E_0\mathcal{A}\tag{40a}$$

$$\bar{\mathcal{H}}_{Ca}=\hat{y}\,\frac{n+\mu_r'\beta}{\mu_r'(1+n\beta)}\frac{E_0}{c\mu_0}\mathcal{A}\tag{40b}$$

$$\bar{\mathcal{P}}_{Ca}=\hat{x}\frac{n^2-\mu_r'}{\mu_r'(1+n\beta)}\frac{E_0}{c^2\mu_0}\mathcal{A}\tag{40c}$$

$$\mu_0\bar{\mathcal{M}}_{Ca}=\hat{y}\frac{n(\mu_r'-1)}{\mu_r'(1+n\beta)}\frac{E_0}{c}\mathcal{A}.\tag{40d}$$

Expressions	Region 0	Region 1	Region 2
$T_{C_{zz}}$	$\frac{E_0^2}{c^2\mu_0}\left(\mathcal{I}^2+\mathcal{R}^2\right)$	$\frac{E_0^2}{c^2\mu_0}\frac{n}{\mu_r'}\left[(c_{ea}\mathcal{A}+c_{ha}\mathcal{B})^2+(c_{eb}\mathcal{A}-c_{hb}\mathcal{B})^2\right]$	$\frac{E_0^2}{c^2\mu_0}\mathcal{T}^2$
G_{C_z}	$\frac{E_0^2}{c^3\mu_0}\left(\mathcal{I}^2-\mathcal{R}^2\right)$	$\frac{E_0^2}{c^3\mu_0}\frac{n}{\mu_r'}\left[(c_{ea}\mathcal{A}+c_{hb}\mathcal{B})(c_{eb}\mathcal{A}-c_{hb}\mathcal{B})\right]$	$\frac{E_0^2}{c^2\mu_0}\mathcal{T}^2$
W_C	$\frac{E_0^2}{c^2\mu_0}\left(\mathcal{I}^2+\mathcal{R}^2\right)$	$\frac{E_0^2}{c^2\mu_0}\frac{n}{\mu_r'}\left[(c_{ea}\mathcal{A}+c_{ha}\mathcal{B})^2+(c_{eb}\mathcal{A}-c_{hb}\mathcal{B})^2\right]$	$\frac{E_0^2}{c^3\mu_0}\mathcal{T}^2$
S_{C_z}	$\frac{E_0^2}{c\mu_0}\left(\mathcal{I}^2-\mathcal{R}^2\right)$	$\frac{E_0^2}{c\mu_0}\frac{n}{\mu_r'}\left[(c_{ea}\mathcal{A}+c_{ha}\mathcal{B})(c_{eb}\mathcal{A}-c_{hb}\mathcal{B})\right]$	$\frac{E_0^2}{c\mu_0}\mathcal{T}^2$

TABLE III. The derived values for the time domain Chu subsystem. The Chu stress tensor and momentum density are expressed in (a) and the Chu power flux and energy density are expressed in (b), for each region of interest.

The time domain Chu fields propagating in the negative direction within the material are

$$\bar{\mathcal{E}}_{Cb}=\hat{x}\,\frac{\mu_r'-n\beta}{\mu_r'(1-n\beta)}E_0\mathcal{B} \tag{41a}$$

$$\bar{\mathcal{H}}_{Cb}=-\hat{y}\,\frac{n-\mu_r'\beta}{\mu_r'(1-n\beta)}\frac{E_0}{c\mu_0}\mathcal{B} \tag{41b}$$

$$\bar{\mathcal{P}}_{Cb}=\hat{x}\frac{n^2-\mu_r'}{\mu_r'(1-n\beta)}\frac{E_0}{c^2\mu_0}\mathcal{B} \tag{41c}$$

$$\mu_0\bar{\mathcal{M}}_{Cb}=\hat{y}\frac{n(\mu_r'-1)}{\mu_r'(1-n\beta)}\frac{E_0}{c}\mathcal{B}. \tag{41d}$$

The transmitted time domain Chu fields are

$$\bar{\mathcal{E}}_{Ct}=\hat{x}E_0\mathcal{T} \tag{42a}$$

$$\bar{\mathcal{H}}_{Ct}=\hat{y}\frac{E_0}{c\mu_0}\mathcal{T}. \tag{42b}$$

For brevity, we define the Chu field coefficients as $c_{ea}\equiv(\mu_r'+n\beta)/(\mu_r'(1+n\beta))$, $c_{ha}\equiv(n+\mu_r'\beta)/(\mu_r'(1+n\beta))$, $c_{eb}\equiv(\mu_r'-n\beta)/(\mu_r'(1-n\beta))$, and $c_{hb}\equiv(n-\mu_r'\beta)/(\mu_r'(1-n\beta))$, which are used in Table III.

The Chu stress tensor, momentum density, energy density, and power flux are utilized to derive the the values for the time varying force and power for the electromagnetic subsystem. Eqs.(29) and (30) are used to derive the electromagnetic force and power in terms provided by the Chu formulation. Table III provides the derived values for calculating the desired time varying electromagnetic force and power contributions.

The time varying Chu electromagnetic force is given as

$$\begin{aligned}\bar{F}_C=&\,\hat{z}\frac{E_0^2}{c^2\mu_0}[(\mathcal{I}^2+\mathcal{R}^2-\mathcal{T}^2)-\beta\{\mathcal{I}^2-\mathcal{R}^2-\mathcal{T}^2\}]\\&+\hat{z}\frac{E_0^2}{c^3\mu_0}\frac{n}{\mu_r'}\Bigg\{v\big[(c_{ea}A(z_1^+)+c_{eb}B(z_1^+))\\&\times(c_{ha}A(z_1^+)-c_{hb}B(z_1^+))\big]-v\big[(c_{ea}A(z_2^+)+c_{eb}B(z_2^+))\\&\times(c_{ha}A(z_2^+)-c_{hb}B(z_2^+))\big]-c_{ea}c_{eb}\int_{R_1}dz\frac{\partial\mathcal{A}^2}{\partial t}\\&+(c_{ea}c_{hb}-c_{eb}c_{ha})\int_{R_1}dz\frac{\partial\mathcal{A}\mathcal{B}}{\partial t}+c_{ha}c_{hb}\int_{R_1}dz\frac{\partial\mathcal{B}^2}{\partial t}\Bigg\}.\end{aligned} \tag{43}$$

where subscript C denotes the Chu electromagnetic subsystem. Here, we note that $\bar{F}_{R_0}=\bar{F}_{R_2}=0$ as previously specified, rendering Eq.(43) as the electromagnetic force within and at the boundaries of the given medium. The time varying Chu electromagnetic power is given as

$$\begin{aligned}P_C=&\,\frac{E_0^2}{c\mu_0}[(\mathcal{I}^2-\mathcal{R}^2-\mathcal{T}^2)+\beta\{\mathcal{I}^2+\mathcal{R}^2-\mathcal{T}^2\}]\\&+\frac{E_0^2}{c^2\mu_0}\frac{n}{\mu_r'}\Bigg\{v\left(c_{ea}A(z_1^+)+c_{eb}B(z_1^+)\right)^2\\&-v\left(c_{ha}A(z_2^-)-c_{hb}B(z_2^-)\right)^2-(c_{ea}^2+c_{ha}^2)\\&\times\int_{R_1}dz\frac{\partial\mathcal{A}^2}{\partial t}-2(c_{ea}c_{eb}-c_{ha}c_{hb})\int_{R_1}dz\frac{\partial\mathcal{A}\mathcal{B}}{\partial t}\\&-(c_{eb}^2+c_{hb}^2)\int_{R_1}dz\frac{\partial\mathcal{B}^2}{\partial t}\Bigg\}.\end{aligned} \tag{44}$$

where $P_{R_0}=P_{R_1}=0$ as shown. Here, due to the sophistication of the terms involved, it is more practical and equally valid to plot the conservation relations $\bar{F}\cdot\bar{v}=P$, and is shown in Fig 4. As is observed, the Chu formulation doesn't satisfy the work-energy theorem for the electromagnetic subsystem. This is due to the respective electromagnetic fields interacting with the optical medium causing a portion of the electromagnetic energy to transfer to the material. This induces the Chu effective charges and currents to oscillate with respect to the presented field relations, producing both kinetic and potential energies within the material [22, 23]. Consequently, this causes the electromagnetic force to deform the material, allowing for the electromagnetic work-energy relation to break down. Thus, the electromagnetic energy transferred to the oscillating dipoles causes the observed differences between the force and power expressions. At any point in time, the work done on the material is less than the kinetic energy delivered to the medium as seen in Fig 4.

IV. DISCUSSION

In Sec. III, we analyze the electromagnetic force and power produced via conservation principles on a moving, linear, lossless, and nondispersive magneto-dielectric slab of material. Both time average and time varying analyses are used to study the electromagnetic-material interaction with respect to a moving frame. In both cases, the

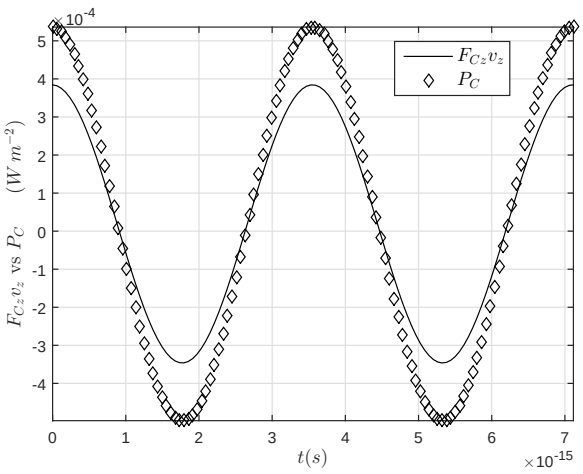

FIG. 4. The graphical representation of conservation, $\bar{F}_C \cdot \bar{v} = P_C$, in terms of the Chu formulation. Here, $\epsilon = 5\epsilon_0$, $\mu = 3\mu_0$, $n = c\sqrt{\epsilon\mu}$, $\lambda_0 = 640nm$, $d = \lambda_0/4n$, and the velocity of the slab is $\bar{v} = \hat{z}7c/10$.

field-kinetic (Chu) and canonical (Minkowski) formulations were applied to interpret the electromagnetic and material subsystems within the moving frame, thereby allowing for an analytic study of optical forces within moving materials. In this section, we review previous works while relating the present contributions to the optical momentum debate. With this, we logically discuss the interpretations of the two electromagnetic subsystems, thereby providing support for the presented analysis.

In the 1950's and 1960's, electromagnetic energy and momentum was employed for the study of a moving dielectric halfspace [24] and a moving slab of material [8]. The former utilized the canonical (Minkowski) formulation to study obliquely incident electromagnetic wave interactions incident on a moving dielectric material. The analysis utilized energy relations of the Doppler shifted incident, reflected, and transmitted waves, along with conservation theorems ($\bar{F} \cdot \bar{v} = P$) to prove validation of the electromagnetic system. The latter experiment utilized the dynamics of the kinetic system as a pulse of light propagates through a material with no reflections, thereby demonstrating momentum conservation and center-of-mass theorems. Within the analysis contained herein, we combine both methods in presenting the relativistic electrodynamics of the kinetic and canonical systems. Here, we note that in modeling magnetodielectric materials, the Amperian formulation [1] differs from the kinetic model, and the related analysis is relegated to a later correspondence. Additionally, the Einstein-Laub and Abraham formulations have both been shown to be invalid with respect to relativistic systems, and have consequently been omitted [5, 25].

First considering the time average analysis, the electromagnetic force and power expressions were shown to be valid and independent of the formulation used; This invokes that the time average force and power results, Eqs. (23) and (24), are correct, yet ambiguous. In viewing the total force density,

$$\langle \bar{f}_{total} \rangle = \nabla \cdot \left\{ \langle \bar{\bar{T}}_{elec} \rangle + \langle \bar{\bar{T}}_{mat} \rangle + \langle \bar{\bar{T}}_{mech} \rangle \right\} + \frac{\partial}{\partial t} \left\{ \langle \bar{G}_{elec} \rangle + \langle \bar{G}_{mat} \rangle + \langle \bar{G}_{mech} \rangle \right\}, \quad (45)$$

it is seen that there are three main contributions to the overall system, where $\langle \bar{\bar{T}}_{elec} \rangle$ and $\langle \bar{G}_{elec} \rangle$ are the electromagnetic stress tensor and momentum density, $\langle \bar{\bar{T}}_{mat} \rangle$ and $\langle \bar{G}_{mat} \rangle$ are the material stress tensor and momentum density, and $\langle \bar{\bar{T}}_{mech} \rangle$ and $\langle \bar{G}_{mech} \rangle$ are the mechanical stress tensor and momentum density, respectively. Modeling the total system while utilizing any electrodynamic formulation allows for different values to be partitioned into the field and material subsystems. However important, the material dependent field expressions (*i.e.* the field and material contributions within the slab) represented by the field-kinetic and canonical formulations [1, 5] produce corresponding equal and opposite forces within the material and at each boundary, thereby canceling to leave no mathematical ability to differentiate between the differing electromagnetic interpretations within the time average analysis. Consequently, this yields trivial results for studying the differences between the field-kinetic and canonical subsystems within the material, where the contributions from the material subsystem define the differences between the field-kinetic and canonical interpretations. This asserts that the time average material subsystem,

$$\langle \bar{f}_{mat} \rangle = \nabla \cdot \left\{ \langle \bar{\bar{T}}_{mat} \rangle \right\} + \frac{\partial}{\partial t} \left\{ \langle \bar{G}_{mat} \rangle \right\} = 0 \quad (46)$$

must render a null net force value. Physically, this implies that however one idealizes and/or models the material subsystem, the time average material contribution adds no value to the moving slab system when considering a lossless material.

To study the electromagnetic interactions within the material, the plane wave field expressions were transformed to the time domain, thereby allowing for an analytical study of the system with respect to both space and time. First studied, the canonical (Minkowski) system demonstrates valid global energy and momentum conservation laws. Mathematically,

$$\nabla \cdot \left\{ \bar{\bar{T}}_M + \bar{\bar{T}}_{mech} \right\} + \frac{\partial}{\partial t} \left\{ \bar{G}_M + \bar{G}_{mech} \right\} = \nabla \cdot \left\{ \bar{\bar{T}}_{elec} + \bar{\bar{T}}_{mat} + \bar{\bar{T}}_{mech} \right\} + \frac{\partial}{\partial t} \left\{ \bar{G}_{elec} + \bar{G}_{mat} + \bar{G}_{mech} \right\} = 0, \quad (47)$$

this imposes that the canonical subsystem includes all electromagnetic and material responses/interactions to close the system, where subscript M denotes the Minkowski electromagnetic formulation. For the field-kinetic formulation, however, conservation of energy and momentum wasn't satisfied, and is due to the separations

of field and material contributions within the electromagnetic subsystem, where the time varying field-kinetic material contribution is a non-zero value. As is observed in Fig 4, the graphical difference between the two respective plots demonstrate the differences between the field-kinetic force and power expressions. Physically, this indicates that the electromagnetic work supplied by the field-kinetic system is not equal to the rate of the energy used by the field-kinetic system. This invokes that the field-kinetic portion of the total electromagnetic force and power can be separated to be used on/deform the material. However, the remaining portion of total electromagnetic force and power defines the material subsystem, and is proportional to the material constitutive parameters. As a result, within the time varying field-kinetic formulation, the force density expression,

$$\nabla \cdot \left\{ \bar{\bar{T}}_{F_k} + \bar{\bar{T}}_{mech} \right\} + \frac{\partial}{\partial t} \left\{ \bar{G}_{F_k} + \bar{G}_{mech} \right\} = -\nabla \cdot \left\{ \bar{\bar{T}}_{mat} \right\} - \frac{\partial}{\partial t} \left\{ \bar{G}_{mat} \right\} \neq 0, \quad (48)$$

demonstrates the necessary conditions for satisfying global conservations laws, where subscript F_k denotes the respective field-kinetic (Chu) formulation. This demonstrates that one may partition the field and material contributions in any way as long as each contribution sums to satisfy Maxwell's equations, reasserting the view in Ref [18]. However, when differentiating material contributions within a given system, there are unique force and momentum expressions linked to specific power and energy expression, which satisfy relativistic electromagnetic theory [5, 25, 26].

V. CONCLUSION

In conclusion, the field-kinetic and canonical subsystems of electrodynamics were studied with respect to two leading formulations (Minkowski and Chu) for both time average and time varying cases. The time average analysis yielded vacuum quantities for both the force and power expressions, which resulted in identical relations for each formulation used. Thus, when modeling the system in terms of any formulation, identical system dynamics are produced. This allowed for a general understanding of the time average electromagnetic force and power around a moving slab of material, but rendered nothing towards the understanding of the electromagnetic differences of the formulations inside the material. The time varying results, however, demonstrated the electromagnetic force and power distributions for both field-kinetic and canonical subsystems, where the respective field representations within the material allowed for analytic study of electromagnetic field and material contributions. As was shown, the canonical subsystem satisfied the time varying electromagnetic subsystem, where the kinetic formulations did not. This is due to the partitioning of the material responses, of which, where not included in the global conservation statement. The methods shown serve to provide a deeper understanding into the field-kinetic subsystem, and illustrate the mathematical framework for dealing with continuum electromechanical systems.

ACKNOWLEDGMENTS

We acknowledge partial support from the National Science Foundation EECS Division of Electrical, Communications, and Cyber Systems (Award No. EECS-1150514) and the Center for Advanced Surface Engineering, under the National Science Foundation Grant No. IIA-1457888 and the Arkansas EPSCoR Program, ASSET III. Any opinions, findings, and conclusions or recommendations expressed in this material are those of the author(s) and do not necessarily reflect the views of the National Science Foundation.

Appendix A: Transformation of complex wave oscillation values

To analyze the time-varying system, we expand the complex field values into the time-varying fields by use of the definition [20]

$$\bar{\mathcal{E}}(z,t) = \mathfrak{Re}\left\{ \bar{\mathcal{E}}(z,\omega) \right\}, \quad (A1)$$

where $\bar{\mathcal{E}}(z,\omega)$ represents values from the complex electromagnetic field relations used in the Sec III A. Here, it is found that the complex exponential and the respective wave coefficients are the only terms to change within the field expressions. Thus, we expand each complex oscillation and wave coefficient terms for each respective wave. As a result,

$$\mathcal{I} = \cos(k_i z - \omega_i t) \quad (A2)$$
$$\mathcal{R} = R_R \cos(k_r z + \omega_r t) + R_I \sin(k_r z + \omega_r t) \quad (A3)$$
$$\mathcal{A} = A_R \cos(k_a z - \omega_a t) - A_I \sin(k_a z - \omega_a t) \quad (A4)$$
$$\mathcal{B} = B_R \cos(k_b z + \omega_b t) + B_I \sin(k_r z + \omega_b t) \quad (A5)$$
$$\mathcal{T} = T_R \cos(k_t z - \omega_t t) - T_I \sin(k_t z - \omega_t t) \quad (A6)$$

are the associated oscillation term for each respective field solution. Here, subscript R and I denote the real and imaginary values of the respective field coefficients. Thus, the real and imaginary wave coefficients derived

from Eqs.(18) yield

$$R_R = \frac{(\beta-1)\left(n^4-\mu_r^4\right)(\cos(\theta)-1)}{(\beta+1)\left(n^2-\mu_r^2\right)^2\cos(\theta)-(\beta+1)\left(n^4+6n^2\mu_r^2+\mu_r^4\right)} \quad \text{(A7a)}$$

$$R_I = -\frac{2n(\beta-1)\mu_r(n-\mu_r)(n+\mu_r)\sin(\theta)}{(\beta+1)\left(n^4-\left(n^2-\mu_r^2\right)^2\cos(\theta)+6n^2\mu_r^2+\mu_r^4\right)} \quad \text{(A7b)}$$

$$A_R = \frac{2\mu_r(n\beta+1)(n+\mu_r)\left((n+\mu_r)^2-(n-\mu_r)^2\cos(\theta)\right)}{(\beta+1)\left(-2\left(n^2-\mu_r^2\right)^2\cos(\theta)+(n-\mu_r)^4+(n+\mu_r)^4\right)} \quad \text{(A7c)}$$

$$A_I = \frac{2\mu_r(n\beta+1)(n-\mu_r)^2(n+\mu_r)\sin(\theta)}{(\beta+1)\left(-2\left(n^2-\mu_r^2\right)^2\cos(\theta)+(n-\mu_r)^4+(n+\mu_r)^4\right)} \quad \text{(A7d)}$$

$$B_R = \frac{2\mu_r(1-n\beta)(n-\mu_r)\left((n+\mu_r)^2\cos(\theta)-(n-\mu_r)^2\right)}{(\beta+1)\left(-2\left(n^2-\mu_r^2\right)^2\cos(\theta)+(n-\mu_r)^4+(n+\mu_r)^4\right)} \quad \text{(A7e)}$$

$$B_I = \frac{2\mu_r(1-n\beta)(n-\mu_r)(n+\mu_r)^2\sin(\theta)}{(\beta+1)\left(-2\left(n^2-\mu_r^2\right)^2\cos(\theta)+(n-\mu_r)^4+(n+\mu_r)^4\right)} \quad \text{(A7f)}$$

$$T_R = \frac{4n\mu_r\left((n+\mu_r)^2\cos(\sigma_A)-(n-\mu_r)^2\cos(\theta-\sigma_A)\right)}{-2\left(n^2-\mu_r^2\right)^2\cos(\theta)+(n-\mu_r)^4+(n+\mu_r)^4} \quad \text{(A7g)}$$

$$T_I = \frac{4n\mu_r\left((n-\mu_r)^2\sin(\theta-\sigma_A)+(n+\mu_r)^2\sin(\sigma_A)\right)}{-2\left(n^2-\mu_r^2\right)^2\cos(\theta)+(n-\mu_r)^4+(n+\mu_r)^4} \quad \text{(A7h)}$$

where σ_A and θ are previously defined, and $X = X_R + iX_I$ utilize standard complex form, where $X \equiv \{R, T, A, B\}$.

[1] B. A. Kemp, J. Appl. Phys **109**, 111101 (2011).
[2] H. Minkowski, Nachr. Ges. Wiss. Göttingen **1**, 53 (1908).
[3] M. Abraham, Rend. Pal. **28**, 1 (1909).
[4] S. M. Barnett, Phys. Rev. Lett. **104**, 070401 (2010).
[5] C. J. Sheppard and B. A. Kemp, Physical Review A **93**, 013855 (2016).
[6] B. A. Kemp and T. M. Grzegorczyk, Opt. Lett. **36**, 493 (2011).
[7] P. Penfield and H. A. Haus, *Electrodynamics of Moving Media* (M.I.T. Press, Cambridge, MA, 1967).
[8] N. Balazs, Physical Review **91**, 408 (1953).
[9] A. Ashkin, Phys. Rev. Lett. **24**, 156 (1970).
[10] J. P. Gordon, Phys. Rev. A **8**, 14 (1973).
[11] M. Mansuripur, Opt. Express **12**, 5375 (2004).
[12] D. F. Nelson, Phys. Rev. A **44**, 3985 (1991).
[13] R. V. Jones and J. C. S. Richards, Proc. R. Soc. Lond. A. **221**, 480 (1954).
[14] R. V. Jones and B. Leslie, Proc. R. Soc. Lond. A. **360**, 347 (1978).
[15] P. Daly and H. Gruenberg, Journal of Applied Physics **38**, 4486 (1967).
[16] R. Peierls, Proc. R. Soc. Lond. A. **347**, 475 (1976).
[17] R. Loudon, J. Mod. Opt. **49**, 821 (2002).
[18] R. N. C. Pfeifer, T. A. Nieminen, N. R. Heckenberg, and H. Rubinsztein-Dunlop, Rev. Mod. Phys. **79**, 1197 (2007).
[19] B. A. Kemp, Progress in Optics **60**, 437 (2015).
[20] J. A. Kong, *Electromagnetic Wave Theory* (EMW Publishing, Cambridge, MA, 2005).
[21] C. J. Sheppard and B. A. Kemp, Physical Review A **89**, 013825 (2014).
[22] B. A. Kemp, J. A. Kong, and T. M. Grzegorczyk, Phys. Rev. A **75**, 053810 (2007).
[23] R. Loudon, L. Allen, and D. F. Nelson, Phys. Rev. E **55**, 1071 (1997).
[24] P. Daly and H. Gruenberg, J. Appl. Phys. **38**, 4486 (1967).
[25] V. G. Veselago and V. V. Shchavlev, Physics-Uspekhi **53**, 317 (2010).
[26] C. Wang, Journal of Modern Physics **4**, 1140 (2013).